Role of the blocking capacitor in control of ion energy distributions in pulsed capacitively coupled plasmas sustained in $Ar/CF_4/O_2$

Sang-Heon Song[a)]
Department of Nuclear Engineering and Radiological Sciences, University of Michigan, 2355 Bonisteel Boulevard, Ann Arbor, Michigan 48109-2104

Mark J. Kushner[b)]
Department of Electrical Engineering and Computer Science, University of Michigan, 1301 Beal Avenue, Ann Arbor, Michigan 48109-2122

(Received 1 November 2013; accepted 21 January 2014; published 4 February 2014)

In plasma etching for microelectronics fabrication, the quality of the process is in large part determined by the ability to control the ion energy distribution (IED) onto the wafer. To achieve this control, dual frequency capacitively coupled plasmas (DF-CCPs) have been developed with the goal of separately controlling the magnitude of the fluxes of ions and radicals with the high frequency (*HF*) and the shape of the IED with the low frequency (*LF*). In steady state operation, plasma properties are determined by a real time balance between electron sources and losses. As such, for a given geometry, pressure, and frequency of operation, the latitude for controlling the IED may be limited. Pulsed power is one technique being investigated to provide additional degrees of freedom to control the IED. In one configuration of a DF-CCP, the *HF* power is applied to the upper electrode and *LF* power is applied to the lower electrode which is serially connected to a blocking capacitor (BC) which generates a self dc-bias. In the steady state, the value of the dc-bias is, in fact, constant. During pulsed operation, however, there may be time modulation of the dc-bias which provides an additional means to control the IED. In this paper, IEDs to the wafer in pulsed DF-CCPs sustained in $Ar/CF_4/O_2$ are discussed with results from a two-dimensional plasma hydrodynamics model. The IED can be manipulated depending on whether the *LF* or *HF* power is pulsed. The dynamic range of the control can be tuned by the dc-bias generated on the substrate, whose time variation depends on the size of the BC during pulsed operation. It was found that high energy ions can be preferentially produced when pulsing the *HF* power and low energy ions are preferentially produced when pulsing the *LF* power. A smaller BC value which allows the bias to follow the change in charged particle fluxes produces a larger dynamic range with which to control IEDs. © *2014 American Vacuum Society*. [http://dx.doi.org/10.1116/1.4863948]

I. INTRODUCTION

The ion energy distribution (IED) is an important control variable in plasma materials processing, especially for high aspect ratio (HAR) etching during microelectronics fabrication.[1] Maintaining the critical dimension, such as a specified angle of the side wall, during etching without reducing the etch rate requires optimizing the IED. A number of strategies have been developed to achieve this goal, including manipulating the shape of bias voltage waveform,[2] applying multiple frequencies,[3] and pulsing either or both of the power supplies when using multiple frequencies.[4–8]

A common strategy for controlling IEDs is employing separate power supplies, typically called the source power and the bias power. The source power is intended to control electron kinetics in the plasma and so control the magnitude of ion and radical fluxes to the wafer. This power is typically applied inductively at many to tens of MHz, as microwave power; or in capacitively coupled plasmas (CCPs) as a high frequency (*HF*) source (10s to 100s MHz). All of these means of applying the source power preferentially heat electrons compared to ions. The bias power is typically applied to the substrate on which the wafer sits in order to control the energy of ions incident onto the wafer, and typically has a lower radio frequency (rf), a few to 10 MHz. With an rf bias power on the substrate, a dc self-bias is often naturally generated in order to produce equal currents flowing into both sides of a series capacitance in the circuit. This series capacitance consists of the wafer, stray capacitance, and a blocking capacitor (BC) in the circuit. The distribution of ion energies bombarding the wafer is then determined by the time variation in the plasma potential produced by the source power, the rf sheath potential generated by the bias power, and the dc-bias on the series capacitance.

A number of strategies have been pursued to control the self-generated dc-bias on the rf driven electrode of CCPs, including variation of the pressure,[9] use of a variable resistor in series with the electrode,[10] and manipulation of the rf bias power[11] or voltage.[12] Many of these prior works focused on the controlling the average ion energy. However, in many applications, such as HAR etching, the ability to control the shape of the IED rather than only the average ion energy is more likely to produce the desired etching profile. In this regard, Qin *et al*. investigated control of the peak energy of the IED and the separation of the peak energies in bimodal

a)Electronic mail: ssongs@umich.edu
b)Author to whom correspondence should be addressed; electronic mail: mjkush@umich.edu

IEDs using nonsinusoidal bias waveforms.[2] They demonstrated the ability to predictably produce arbitrary IEDs at selected energies by tailoring the shape of the bias voltage waveform.

In continuous wave (*cw*) operation, the plasma must exactly balance the source of electrons and losses of electrons averaged over the rf period. In single frequency operation of CCPs, for a given set of operating conditions (pressure, gas mixture, flow rate power deposition, and frequency), there is usually a single voltage amplitude that will satisfy this balance. For multifrequency CCPs, there is additional latitude but not unlimited latitude. As a result, in *cw* operation, the ability to control of the IED is constrained by these balance requirements. One of the advantages of pulsed power operation is that the electron sources and losses need only be balanced averaged over the pulsed cycle, which can be as long as many ms. As a result, additional control parameters are introduced, such as pulse repetition frequency (PRF) and duty-cycle. (PRF is the number of times per second that the pulse power waveform is repeated and the duty-cycle is the fraction of the pulse period that the power is on.) Agarwal *et al.*[4] investigated the temporal dynamics of charged species using pulse power in a multifrequency CCP by varying PRF. In order to refine the control of ion fluxes to the substrate, they computed not only the plasma potential, but also the self-generated dc-bias across the blocking capacitor in the presence of pulse power on either one of the electrodes. They found that the dc-bias had time variation during the pulse period that is delayed due to the charging of the blocking capacitor.

Maeshige *et al.*[13] investigated the fluxes of charged species in a dual frequency CCP (DF-CCP) with a 1 MHz *cw* bias and a pulsed 100 MHz source in a $Ar/CF_4 = 95/5$ mixture at 50 mTorr. They found that the self-bias oscillated during the pulse period (20 μs) where each of the electrodes was capacitively coupled through a blocking capacitor of 0.5 nF. They also demonstrated control of the incident fluxes of electrons as well as the positive and negative ions onto the wafer during the power on and off phases as a function of time. Experiments by Ohmori *et al.*[14] showed similar trends, including negative ion generation during the afterglow.

In this paper, we build on these prior works by discussing results from a computational investigation of ion energies produced in pulsed DF-CCPs sustained in a $Ar/CF_4/O_2$ when varying the blocking capacitance. We found that ion energies averaged over the pulsed period extend to higher values when pulsing the *HF* power compared to pulsing the low frequency (*LF*). Depending on the size of the BC, the self-generated dc-bias voltage may be modulated during the pulse period. As a result, the IED incident onto the wafer may be a function of the size of BC during pulsed operation. Varying the size of BC then provides an additional means for controlling the IED.

The model used in this study is described in Sec. II. The plasma properties in pulsed DF-CCPs are discussed in Sec. III, and the control of the IED is discussed in Sec. IV. Our concluding remarks are in Sec. V.

II. DESCRIPTION OF THE MODEL

The model used in this investigation is a two-dimensional fluid hydrodynamics simulation, the Hybrid Plasma Equipment Model (HPEM), which combines separate modules which address different physical phenomena.[15] The modules used in this study are the Electron Energy Transport Module (EETM), the fluid kinetics-Poisson module (FKPM), and the Plasma Chemistry Monte Carlo Module (PCMCM). In the FKPM, separate continuity, momentum, and energy equations are simultaneously integrated in time for all heavy particle species (neutral and charged). Using drift-diffusion fluxes derived using the Sharffeter–Gummel formulation,[16] continuity equations are integrated for electrons. These equations are solved coincident with a semi-implicit solution of Poisson's equation.

All electron transport coefficients and rate coefficients for electron impact collisions are provided by the EETM using an electron Monte Carlo simulation (eMCS).[17] The electric fields binned as a function of rf phase produced by the FKPM are interpolated for position and time in the EETM. Two sets of calculations are performed in the eMCS—one for bulk electrons and one for secondary electrons emitted from electrodes in response to ion bombardment.

The FKPM and EETM are sequentially and iteratively called during execution of the model. The time spent in the FKPM is chosen to be a small fraction of the pulsed period so that the electron transport and rate coefficients are frequently updated. In a typical run of the model, a 6–12 pulsed periods are computed to achieve a pulse-periodic steady state. Acceleration techniques are used early in the computation to speed the integration toward the quasi-steady state. IEDs and plasma parameters are recorded during the last 1–2 pulse periods.

Since heavy species (charged and neutral) transport is obtained by solving fluid equations in the FKPM, the energy and angular distributions of these species are not directly available. These distributions incident onto the substrate are calculated using Monte-Carlo techniques in PCMCM.[18] The source functions for generation of the ions from all sources (electron impact and heavy particle collisions) and electric fields computed in the FKPM are exported to the PCMCM. Pseudoparticles, representing ions in the PCMCM, are launched during the pulse period at locations weighted by their source functions throughout the plasma volume. The trajectories of the pseudoparticles are integrated by interpolating electric fields in space and time in the same manner as in the eMCS. The gas phase collisional processes of the pseudoparticles are computed based on the same reaction mechanism as in the FKPM. The trajectories of the pseudoparticles are followed until they strike the surface at which time their energy and angular distributions are recorded.

For *cw* excitation, the IEDs of particles striking the wafer are computed after the last iteration of the HPEM. During pulsed operation, statistics are collected over many iterations during the last pulse period in order to resolve IEDs as a function of time during the pulse period. The ion energy and angular distributions are then averaged over the pulse period for display here.

For the DF-CCP investigated here, *HF* power is applied to the upper electrode and *LF* power is applied to the lower electrode on which the wafer sits. A pulse power waveform is specified by the voltage amplitude, PRF, and duty-cycle. It is common in actual operation of a plasma tool to specify the power and adjust the voltage to deliver that power. Unfortunately, doing so makes it difficult to make side-by-side comparisons of IEDs when varying other parameters. So, in this investigation, the voltage is specified for each frequency. In order to resolve the rf cycle of both frequencies, the fundamental time step is chosen to be less than 0.0025 of the highest applied frequency (6.25×10^{-11} s for 40 MHz). The time step may be further reduced to satisfy the Courant limit. Since the solution technique is semi-implicit, there is typically not a constraint on the shorter dielectric relaxation time. Time steps in the PCMCM are dynamically chosen to resolve ion transport in the time varying sheath. The time step is chosen to be no larger than a fraction of the rf cycle (typically 0.01) or the time to cross a fraction of a computational mesh cell (typically 0.5 far from the sheath and 0.02 in the sheath). A blocking capacitor is in series with the *LF* electrode and a time dependent dc-bias is obtained by a real time integration of the collected current. The value of dc-bias is updated every rf cycle of the low frequency (0.1 μs at 10 MHz).

We investigated IEDs onto the wafer in pulsed DF-CCP using an $Ar/CF_4/O_2 = 75/20/5$ gas mixture at 40 mTorr and 200 sccm. The species in the simulation are Ar, Ar^+, Ar(4s) metastable, Ar(4s) radiative, Ar(4p, 5d), CF_4, CF_3, CF_2, CF, C, F, F_2, C_2F_4, C_2F_6, $CF_3{}^+$, $CF_2{}^+$, CF^+, C^+, $F_2{}^+$, F^+, $CF_3{}^-$, F^-, O_2, $O_2(^1\Delta)$, $O_2{}^+$, O, $O(^1D)$, O^+, O^-, COF, COF_2, CO_2, FO, SiF_4, SiF_3, and SiF_2. The reaction mechanism is discussed in Ref. 19. For calculation of the IEDs, all eight ions except for C^+ (negligible concentration) are included in the PCMCM.

III. PLASMA PROPERTIES OF PULSE POWERED DF-CCP SUSTAINED IN $Ar/CF_4/O_2$

The two-dimensional, cylindrically symmetric reactor used in this investigation is schematically shown in Fig. 1(a). The lower electrode serves as the substrate, which is powered at a *LF* of 10 MHz. A conductive Si wafer ($\varepsilon/\varepsilon_0 = 12.0$, $\sigma = 0.01\ \Omega^{-1}\,cm^{-1}$), 30 cm in diameter, sits in electrical contact with the substrate. The upper electrode, 36 cm in diameter, is powered at a *HF* of 40 MHz. The *HF* electrode serves as the shower head through which gas is injected. Both electrodes are surrounded by a dielectric ($\varepsilon/\varepsilon_0 = 8.0$, $\sigma = 10^{-6}\ \Omega^{-1}\,cm^{-1}$). All other surfaces in the reactor are grounded metal including the annular pump port. The gap between the two electrodes is 4 cm. All of the surfaces facing the plasma have the same secondary emission coefficient $\gamma = 0.15$ for ion bombardment.[20] Both electrodes are powered at constant voltage.

A single blocking capacitor is used in the circuit whose value is varied from 10 nF to 1 μF. The range of typical values of blocking capacitors in commercial plasma tools is from a few nF to several hundreds of nF depending on the system size and application. The BC is located between the *LF* electrode and the *LF* power supply source, as shown in Fig. 1(b). The current collected by the *LF* electrode is directed to the plasma facing plate of the BC. The current collected by all other metal surfaces in the reactor is directed through ground to the *LF* power supply facing plate of the BC. In practice, a control surface is placed at the edge of all metal surfaces. The average current over an rf cycle having period τ through that control surface with surface normal $\hat{n}$ to an electrode (or metal material) is then

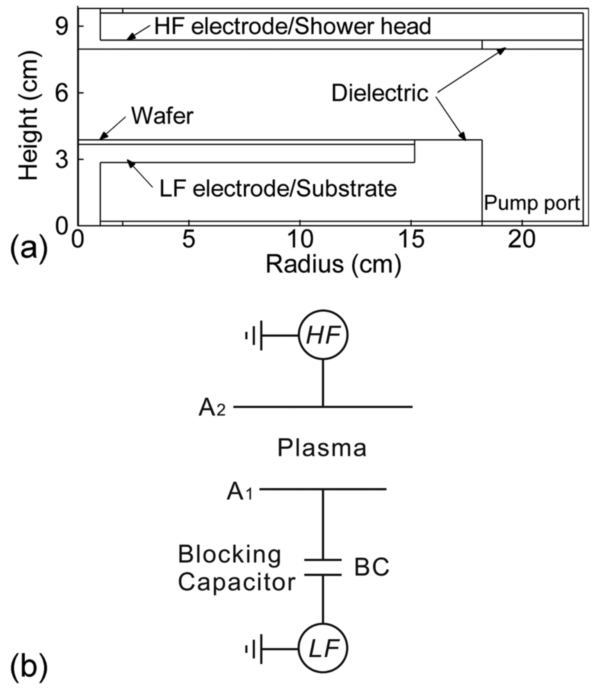

FIG. 1. Operating system for this investigation. (a) Geometry of the DF-CCP chamber. The *LF* (10 MHz) is applied on the lower electrode, and the *HF* (40 MHz) is applied on the upper electrode. One of the two frequencies is operated in pulse mode with a few tens of kHz PRF. (b) Electrical schematic for the DF-CCP system. The BC is connected in series with the lower electrode.

$$\bar{I} = \frac{-1}{\tau}\int_0^{\tau}\left(\sum_i q_i\vec{\phi}_i(1+\gamma_i) + \sum_i q_e\vec{\phi}_i\gamma_i + \varepsilon\frac{d\vec{E}}{dt}\right)\cdot\hat{n}\,dt, \tag{1}$$

where the first sum is over ions (and electrons) having charge q_i, incident flux $\vec{\phi}_i$ and electron secondary electron emission coefficient γ_i, the second sum is for neutral particles and photons producing secondary electrons, and ε is the permittivity in the material adjacent to the metal surface (which may not be plasma). $\hat{n}$ is the normal to the surface. Here, positive current for a given electrode is defined as positive charge flowing into the surface. The currents are collected over a single low frequency cycle and the dc bias is then incrementally updated. This results in discrete changes in the dc bias in the figures discussed below.

The base case operating conditions are 40 mTorr of an $Ar/CF_4/O_2 = 75/20/5$ mixture with the amplitude of both the *LF* (10 MHz) and the *HF* (40 MHz) being 250 V. Either the

LF or *HF* power can be delivered in a pulsed format. The rise (or decay) time of the power-on (or power-off) period is 500 ns. The base case pulsing properties are 50 kHz PRF (pulse period 20 μs) and 25% duty-cycle. For parametric investigations, the PRF was varied from 50 kHz to 250 kHz and the duty-cycle was varied from 25% to 75%. Since two frequencies are applied to separate electrodes, *cw* means that both *HF* and *LF* powers are applied in *cw* mode and *pulsed* means that one of these powers is operated in pulsed mode while the other remains in *cw* mode. In order to isolate the effects of pulsing the *LF* and *HF*, only one of the powers is pulsed at a time.

Electron density, n_e, and electron temperature, T_e, are shown in Fig. 2 at different times during the pulse period for the base case conditions of when pulsing the *HF* power. n_e and T_e are shown in Fig. 3 for pulsing the *LF* power. The modulation of n_e and T_e is greater when pulsing the *HF* power than when pulsing the *LF* power, a consequence of the higher efficiency of electron heating at the higher frequency. When pulsing the *HF*, the maximum n_e increases

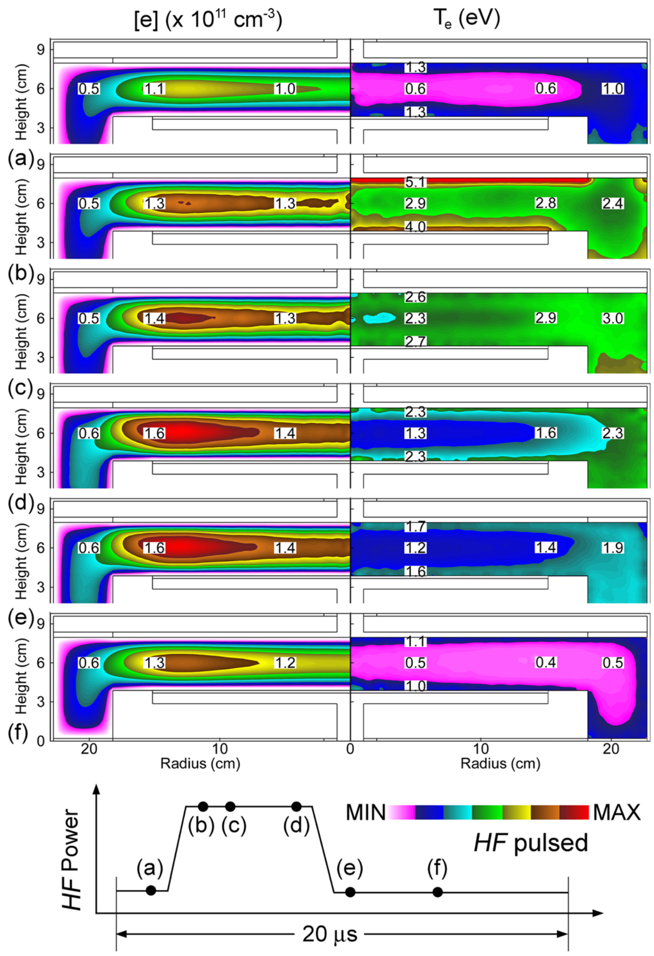

FIG. 2. (Color online) Electron density (left) and temperature (right) when pulsing the *HF* power at different times during the pulsed cycle (as indicated in the lower figure). ($Ar/CF_4/O_2 = 75/20/5$, 40 mTorr, 200 sccm, *LF* = 250 V at 10 MHz *cw*, *HF* = 250 V at 40 MHz in pulse mode with BC = 1 μF, PRF = 50 kHz and 25% duty-cycle.) The electron density is modulated by about 30% during the pulse cycle while the electron temperature shows nearly instantaneous changes as the *HF* power toggles on and off, especially near the sheaths due to enhanced stochastic heating.

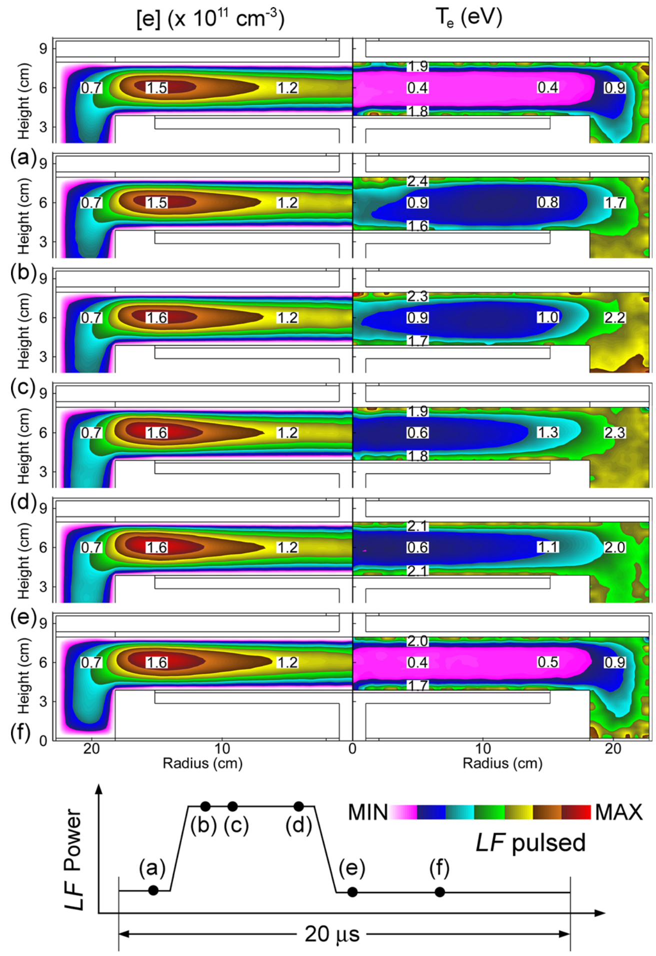

FIG. 3. (Color online) Electron density and temperature when pulsing the *LF* power at different times during the pulsed cycle (as indicated in the lower figure). ($Ar/CF_4/O_2 = 75/20/5$, 40 mTorr, 200 sccm, *LF* = 250 V at 10 MHz in pulse mode with BC = 1 μF, PRF = 50 kHz and 25% duty-cycle, *HF* = 250 V at 40 MHz *cw*.) Pulsing the *LF* power produces nominal intercycle changes in electron density and temperature over the pulse period as the majority of the *LF* power is dissipated in ion acceleration.

from $1.1 \times 10^{11}\,\mathrm{cm}^{-3}$ at the start of the power-on period to $1.6 \times 10^{11}\,\mathrm{cm}^{-3}$ at the end. The more efficient stochastic electron heating by the *HF* raises T_e to 2.9 eV in the bulk and to 5.1 eV in the *HF* sheath. Prior to applying the *HF* power, T_e in the bulk plasma is as low as 0.6 eV and only 1.3 eV adjacent to the sheaths. This value of T_e is enabled, in part, by the continuous background ionization by secondary electrons produced by the *LF* bias. When pulsing the *LF*, n_e remains at $1.5 - 1.6 \times 10^{11}\,\mathrm{cm}^{-3}$ while T_e has only a nominal increase from 0.4 eV to 0.9 eV in the bulk and to 2.4 eV in the sheath.

Pulsing the *HF* produces a more uniform plasma, particularly during the power-on phase. During the *HF* power-off period (when only the *LF* power is on), T_e adjacent to the electrodes is about 1.3 eV, as shown in Fig. 2(a). During *LF* power-off period (when only *HF* power is on), T_e adjacent to the electrodes is about 1.9 eV, as shown in Fig. 3(a). Due to the higher rate of stochastic heating by the *HF*, the T_e during the power-off cycle is larger when pulsing the *LF* (when the *HF* is on) than pulsing the *HF* (when the *LF* is on).

For this reason, the electron density is larger during the *LF* power-off period.

At the start of the power-on cycle, T_e momentarily increases (overshoots) its steady state value. This is due, in part, to the bulk electrons having drifted closer to the electrode during the power off period due to the reduction in the sheath thickness resulting from the lack of the applied voltage. Upon ramp up of the voltage at the start of the power-on phase, these electrons are heated by the progressively expanding sheath thickness. The amount of overshoot is larger with pulsing *HF* as the sheath velocity is higher.

IV. CONTROL OF THE IED IN PULSE POWERED DF-CCP USING BLOCKING CAPACITANCE

Due to the time varying current collected by the electrodes during the pulse period, the spatial variation of the current and the finite size of the BC, the self dc-bias may be modulated during the pulse period. The degree of modulation is determined in large part by the size of the BC. Larger BCs require longer periods to initially charge to a quasi-dc voltage, but then also require a larger differential current to change that voltage. As a result, there is less modulation during the pulse period. Small BCs rapidly charge to their quasi-dc voltage, but that voltage is more sensitive to small changes in differential current. Since the differential current is a function of the pulse power waveform, the time dependence of the dc-bias will also be a function of the pulse power waveform for a given size of the BC.

For example, the plasma potential and voltage on the BC are shown in Fig. 4 when pulsing the *HF* for a PRF of 50 kHz and duty-cycle of 25%. Although difficult to discern in the figure due to plotting resolution, the plasma potential has oscillations at both the *HF* and *LF*. For *cw* excitation, the dc-bias is −48 V. Upon application of *HF* power with a BC of 10 nF, the dc-bias spikes from −100 to 5 V, which accompanies an increase in the plasma potential to 250–275 V. Upon termination of the *HF* power, the dc-bias falls to −200 V before recovering to about −90 V during the afterglow. Note that for this particular set of conditions and for this small value of BC, the dc-bias oscillates between −80 V and −100 V on a *LF* cycle to *LF* cycle basis during the *HF* afterglow. This is an effect that is magnified by the model which changes the dc-bias only on a rf cycle-by-cycle basis. The oscillation is nevertheless indicative of the sensitivity of the dc-bias to the size of the BC. Only the rf-cycle average dc-bias is plotted for clarity by omitting the oscillation during the afterglow period. When the BC is increased to 1 μF, the oscillation of the dc-bias during the pulse period is significantly reduced, in this case to only ±15 V. This difference in behavior of the dc-bias is largely due to the different RC (resistance × capacitance) constant of the circuit. This variation in dc-bias during a pulse period has been noted by Agarwal *et al.*[21]

The plasma potential and voltage on the BC are shown in Fig. 5 when pulsing the *LF* for a PRF of 50 kHz and duty-cycle of 25%. When pulsing the *LF*, the time averaged dc-bias is positive, which implies that the *cw HF* electrode is collecting more current. With the smaller BC (10 nF), the change in current at the onset of the *LF* pulse restores high current collection on the *LF* electrode and results in the dc-bias transitioning from +75 V to −55. (The RC time constant based on resistance of the plasma is about 0.3 μs.) Upon cessation of the *LF* pulse, the dc-bias returns to positive values. With the larger BC (1 μF) and longer RC time constant (about 30 μs), the dc-bias has a smaller amplitude of oscillation. However, the transient lasts almost the entire *LF* pulsed cycle. In either case, in spite of the dynamics of the dc-bias being different, the time averaged dc-bias is nearly independent of the value of the BC. The time averaged dc-bias is 44 V with 10 nF and 47 V with 1 μF.

As a consequence of the different temporal dynamics of the dc-bias and so total bias voltage on the substrate, the IED

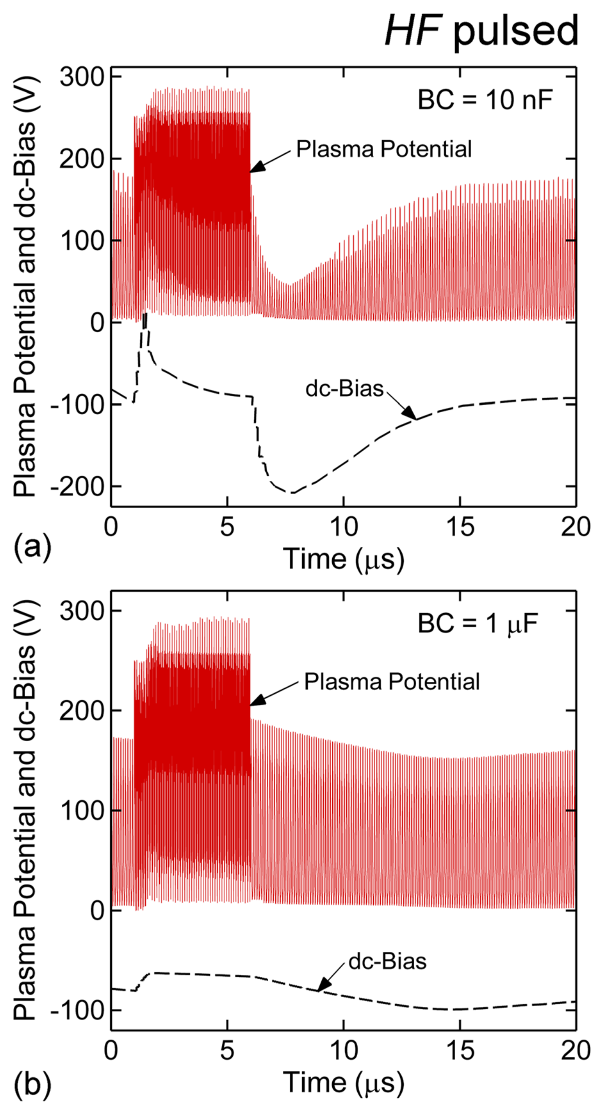

FIG. 4. (Color online) Plasma potential, V_P, and dc-bias, V_{dc}, during one pulse period when pulsing the *HF* power (PRF = 50 kHz, 25% duty-cycle). (a) BC = 10 nF and (b) BC = 1 μF. The sheath potential is $V_S = V_P - V_{dc}$. The *LF* power is always on and the *HF* power is on only during the pulse window of 25%. Due to the smaller RC time constant with the small BC, the dc-bias responds more quickly. Since the voltage amplitude of the *LF* power rides on the dc-bias, the maximum envelope of the plasma potential has the same shape as the dc-bias.

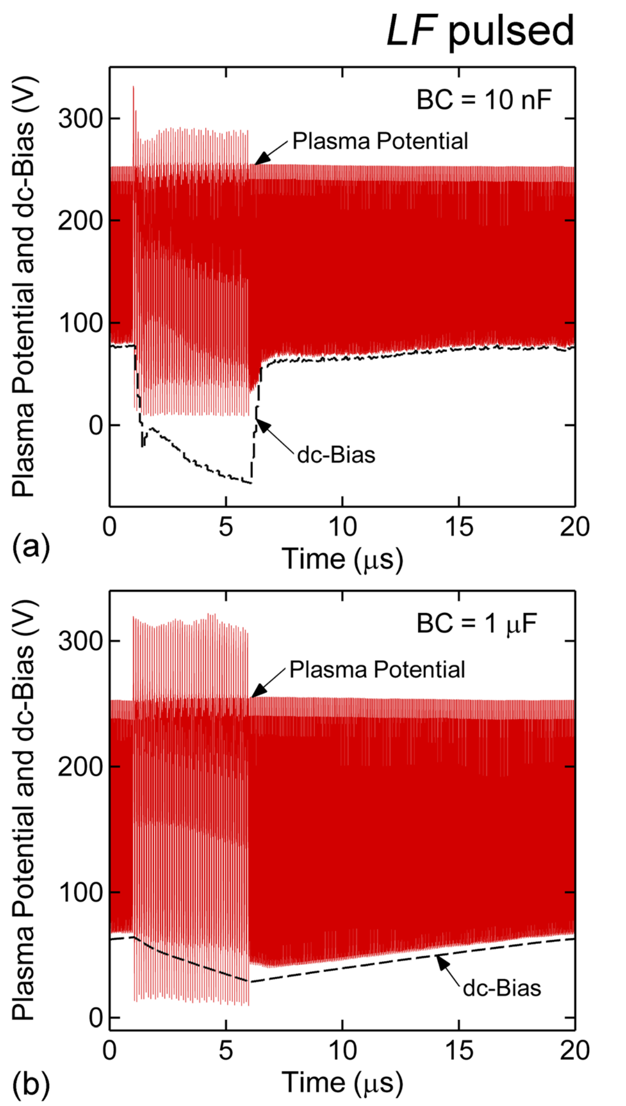

FIG. 5. (Color online) Plasma potential, V_P, and dc-bias, V_{dc}, during one period when pulsing the *LF* power (PRF = 50 kHz, 25% duty-cycle). (a) BC = 10 nF and (b) BC = 1 μF. The sheath potential is $V_S = V_P - V_{dc}$. The *HF* power is always on and the *LF* power is on only during the pulse window of 25%. The plasma potential is mainly determined throughout the pulse period by the voltage amplitude of the *cw HF* power. The dynamic range of dc-bias is larger with the smaller BC.

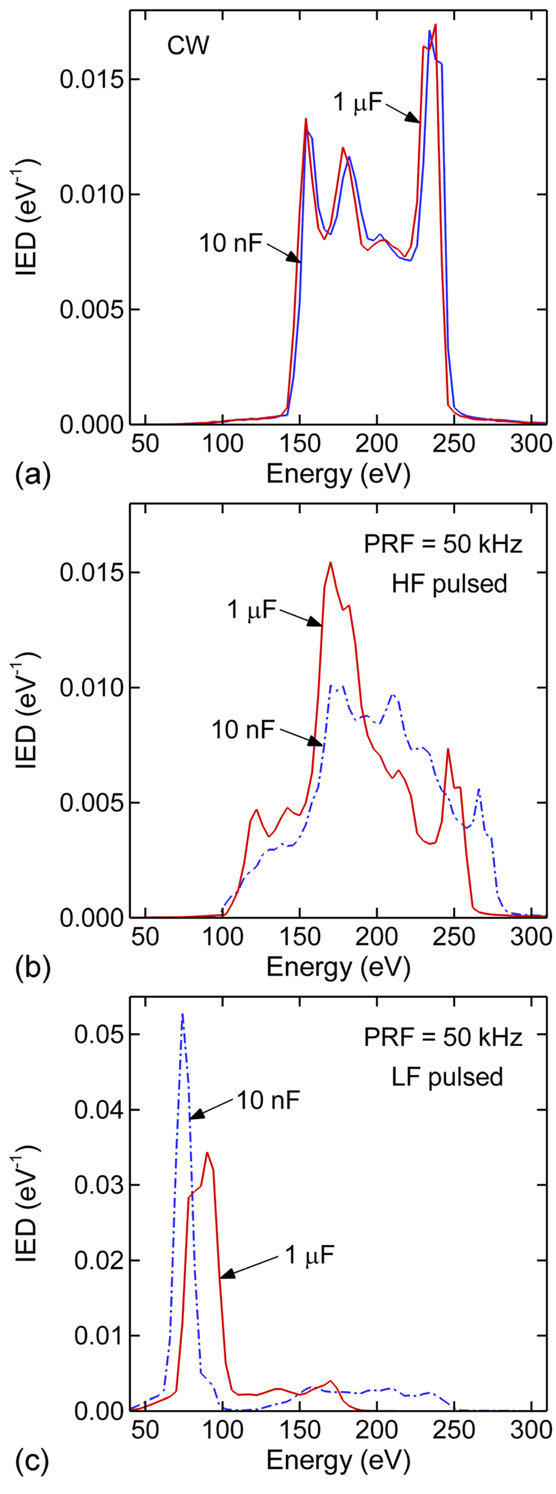

FIG. 6. (Color online) Total IEDs for all ions with different sizes of the BC for the base case (40 mTorr, 250 V at 10 MHz, 250 V at 40 MHz). (a) *cw* operation, (b) pulsing *HF* power, and (c) pulsing *LF* power. Pulsing has a PRF of 50 kHz and 25% duty-cycle. The IED is insensitive to the size of BC with *cw* operation while its shape depends on the size of BC with pulsed operation.

to the substrate averaged over a pulsed cycle is a function of the value of the BC. If the value of the BC is large enough so that the RC time constant is much larger than a single rf period, the dc-bias should be constant and independent of the value of the BC. For example, time averaged IEDs for all ions (including CF_3^+, CF_2^+, CF^+, F_2^+, F^+, O_2^+, O^+, and Ar^+) are shown in Fig. 6(a) for *cw* excitation with a BC of 10 nF and 1 μF. The IED does not have the typical bimodal appearance. This results from the IED being the sum of the individual distributions for ions of different masses, the non-steady dc bias, ions responding to both frequencies and responding to the multifrequency Fourier components resulting from pulsing. These shapes are discussed below. The IEDs are insensitive to the size of the BC in *cw* operation since the size of the BC only determines the initial charging time. (We note that it is possible that the dc-bias could vary during a single rf period if the value of the BC is small enough; however, that is typically not the case in industrial practice.)

IEDs are shown in Figs. 6(b) and 6(c) for pulsing the *HF* and *LF* for a PRF of 50 kHz. When pulsing the *HF*, the IEDs extend to both higher and lower energy compared to the *cw* cases. The smaller BC produces a larger dynamic range of the IED, reaching a higher energy. Recall that the instantaneous sheath potential on the substrate is approximately $V_S = V_P - V_{dc}$, where V_P is the plasma potential and V_{dc} is the dc-bias. The change in IED behavior has at least two origins. The first is the increase in plasma potential during the *HF* pulse which increases V_S. The increase in plasma potential is both instantaneous and averaged over the rf cycle. The second is the transient in V_{dc} to more negative values which also increases V_S. The dynamic range of the dc-bias is larger with a smaller BC—the lowest dc-bias is −200 V with 10 nF and −100 V with 1 μF. Nevertheless, the maximum ion energy with a BC of 10 nF is 280 eV which is only 20 eV larger than with 1 μF in spite of the dc-bias being 100 V more negative. The dynamics of the plasma potential and dc-bias are such that the most negative dc-bias also occurs when the plasma potential is at its minimum value when only the *LF* is on (see Fig. 4). As a result, $V_S = V_P - V_{dc}$ does not significantly increase during this time. On the other hand, when the *LF* power is pulsed, the opposite scenario occurs.

Pulsing the *LF* power produces a sharp peak at low energy and a broad peak at high energy in the IED. These peaks are sensitive to the BC. The low energy peak results from ions collected from that portion of the pulse period when the *LF* voltage is off and the plasma potential oscillates only at the *HF*. Since the *HF* is above the ion response frequency (ion plasma frequency is about 10 MHz for argon ions and 17 MHz for oxygen ions), a single low energy peak in the IED is produced. The high energy peak results from ions collected during that portion of the pulsed period when the *LF* voltage is on, the plasma potential is larger and the dc-bias is more negative (or less positive). The IED with the smaller BC (10 nF) extends to 250 eV, a consequence of the dc-bias cycling to more negative (or less positive) values, thereby producing a larger V_S. The IED with the larger BC (1 μF) extends to only 180 eV, a consequence of the dc-bias having a smaller dynamic range thereby producing a smaller V_S. The location of the low energy peak is determined by the difference of the *HF* produced plasma potential and dc-bias after the *LF* pulse. Since the smaller BC responds more quickly to the change in plasma properties, the dc-bias is both more negative during the pulse and more positive after the pulse. Therefore, V_S is smaller after the pulse and the IED peaks at lower energy.

Controlling the shape of IED can also be achieved by adjusting the pulse power parameters such as PRF and duty-cycle. The IEDs for all ions with different PRFs are shown in Fig. 7 for large and small BCs when pulsing the *HF* power. The corresponding dc-biases are shown in Fig. 8 as a function of the normalized time, which is time divided by the length of the pulse period. The width of the IED and its shape can be controlled for a given BC by changing PRF—or for a constant PRF, by varying BC. However, the relationship between PRF for a given BC and the maximum ion energy is nonmonotonic. These trends depend on the details of the ions responses to the Fourier components of the bias

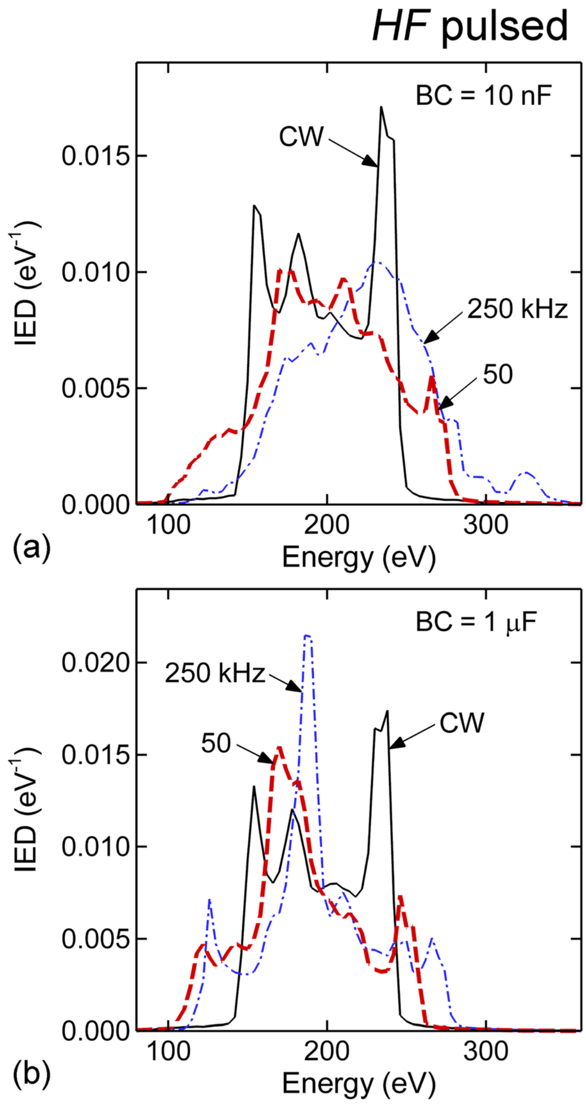

FIG. 7. (Color online) Total IEDs for all ions for different PRFs when pulsing the *HF* power with a 25% duty-cycle. (a) BC = 10 nF and (b) BC = 1 μF. The IED becomes single-peaked in appearance with the smaller BC while the IED maintains a multiple-peaked shape with the larger BC. The IEDs with larger PRFs extend to the higher energies.

that result from the pulsing. For a given PRF, the dc-bias changes over a larger dynamic range during the pulse period with the smaller BC. The heavier ions tend to respond to the time averaged sheath potential and so do not reflect the full dynamic range of the dc-bias. As a result the IED tends to have a single major peak with smaller wings to higher and lower energy. With the larger BC, the dc-bias varies more slowly during the pulse cycle, which enables the heavier ions to respond to the change in V_S, and so produce more structure to the IED.

For a given value of BC, the IEDs tend to have less structure with higher PRF since the heavier ions are not able to respond to the dynamics of the dc-bias during the shorter pulse period. With the smaller BC and smaller RC time constant, the dc-bias spikes at the leading edge of *HF* power-on, as shown in Fig. 8(a). This spike is suppressed at higher PRF due to the shorter interpulse period. With the higher PRF

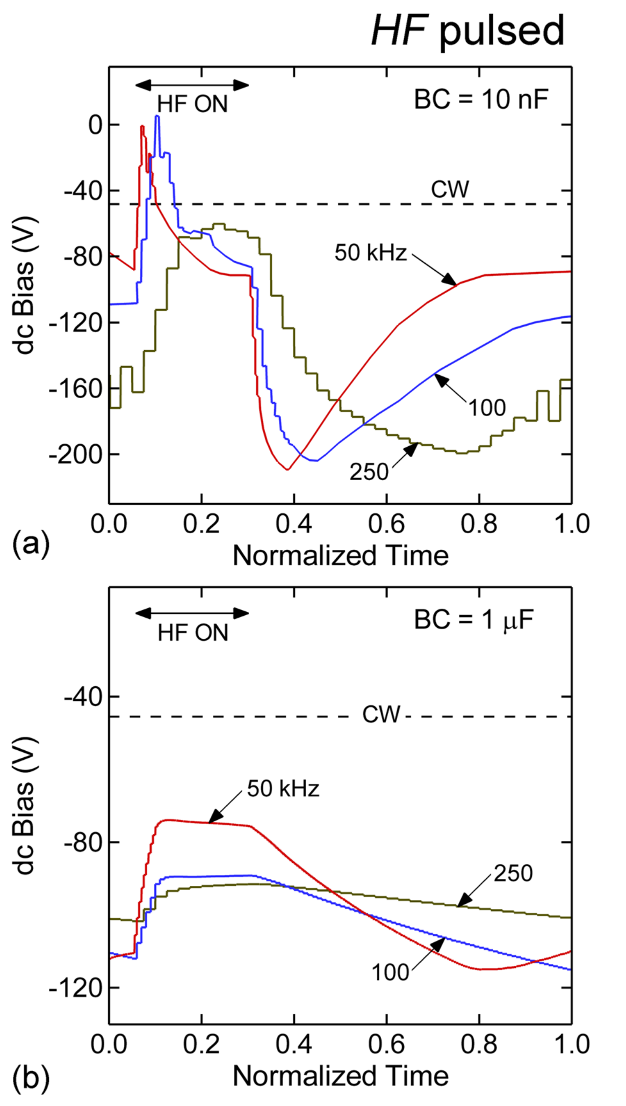

FIG. 8. (Color online) DC-bias as a function of normalized time (which is time divided by the length of each pulse period) with different PRFs when pulsing the *HF* power with a 25% duty-cycle. (a) BC = 10 nF and (b) BC = 1 μF. The *LF* power is *cw*. During power-on period, the dc-bias becomes less negative with some overshoot with smaller PRFs.

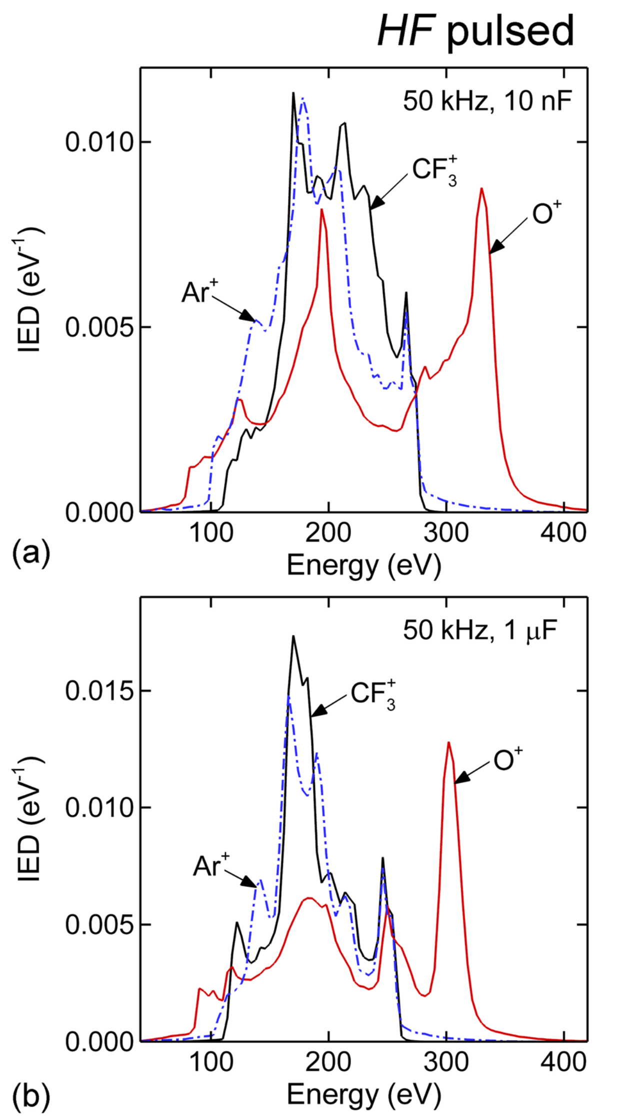

FIG. 9. (Color online) Ion energy distributions for O^+, Ar^+, and $CF_3{}^+$ when pulsing the *HF* power. (a) BC = 10 nF and (b) BC = 1 μF.

and shorter afterglow period, the dc-bias does not have enough time to recover back to what would be a *cw* value. The oscillation of dc-bias during the pulse period decreases as the BC increases due to the larger RC time constant. The magnitude of the oscillation also decreases with larger PRF due to the shorter interpulse period. It is natural to associate the IED obtained with high PRF with the IED obtained with *cw* excitation. While that is certainly true for very high PRF and large values of BC, the dynamics of the dc-bias with small values of BC make the IEDs even for a PRF of 250 kHz significantly different than those of *cw* excitation.

The IEDs for different ions (O^+, Ar^+, and $CF_3{}^+$) are shown in Fig. 9 for small (10 nF) and large (1 μF) BCs when pulsing the *HF* with a PRF of 50 kHz. Due to the different transit times through the sheath, there are differences in the IEDs between O^+, Ar^+, and $CF_3{}^+$. The O^+ (16 amu) has a broader IED compared to $CF_3{}^+$ (69 amu) as its lower mass makes it more sensitive to time dependent variations in the sheath potential. The IEDs for the heavier ions (Ar^+ and $CF_3{}^+$) track each more closely for a given BC. The IED for the lighter ion (O^+) better reflects the maximum and minimum in V_S during the pulse period. A portion of these differences in IEDs is likely due to the source functions of O^+, Ar^+, and $CF_3{}^+$ being different during the pulse period. As a result, these different ions arrive at the sheath edge and are preferentially accelerated into the sheath when the dc-bias has different values.

When pulsing the *LF*, the general shapes of the IEDs are retained when changing PRF, as shown in Fig. 10. The dc-bias for these cases is shown in Fig. 11 as a function of the normalized time. The dynamic range of the oscillation in the dc-bias is from -40 to $+80$ V with the smaller BC (10 nF). The dynamic range with the larger BC (1 μF) is at most $+30$ to $+60$ V. In both cases, the time dependence of the dc-bias is about the same between different PRFs. Consequently, the IEDs are relatively insensitive to the PRF for a given BC. The most significant variation in the IED occurs when

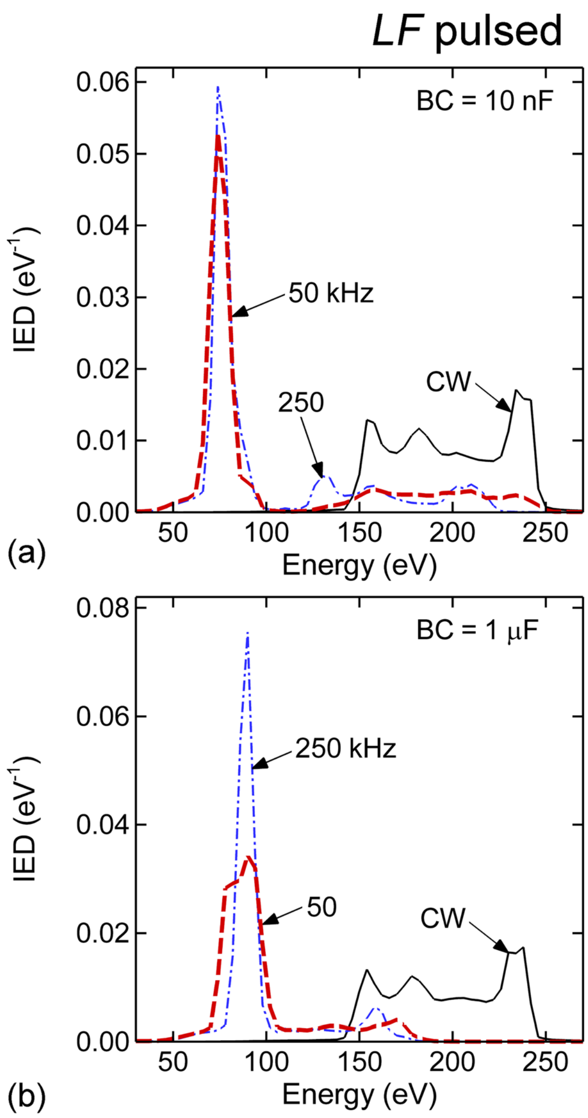

FIG. 10. (Color online) Total IEDs for all ions for different *PRFs* when pulsing the *LF* power with a 25% duty-cycle. (a) BC = 10 nF and (b) BC = 1 μF. The IED extends to higher energies with the smaller BC.

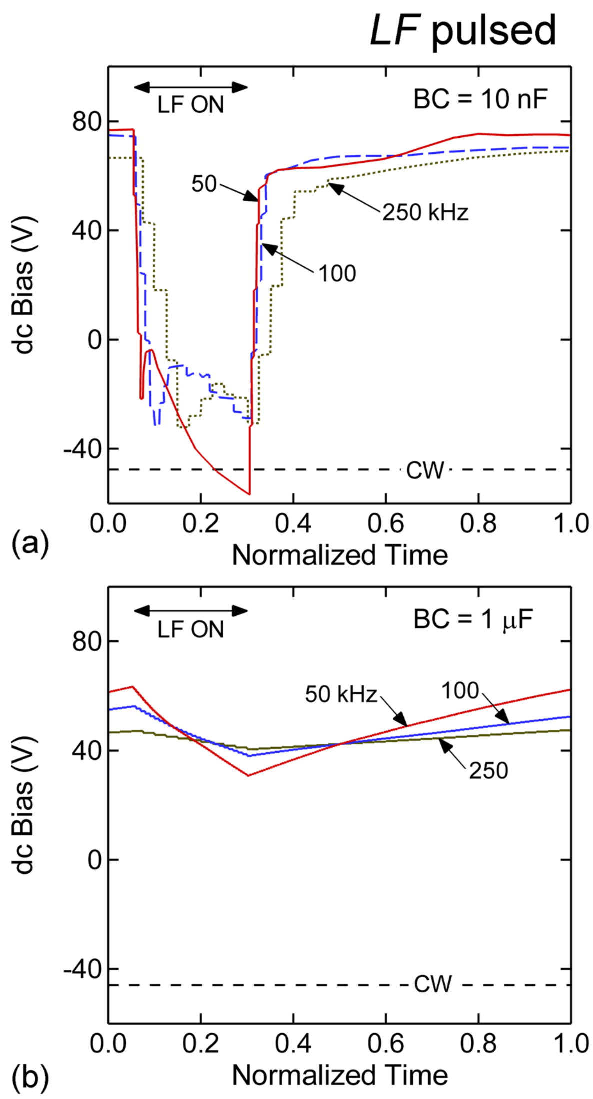

FIG. 11. (Color online) DC-bias as a function of the normalized time (which is time divided by the length of each pulse period) with different PRFs when pulsing the *LF* power with a 25% duty-cycle. (a) BC = 10 nF and (b) BC = 1 μF. The *HF* power is *cw*. If the size of BC is small enough for the dc-bias to response to the voltage on the electrode, the temporal behavior of dc-bias is similar for different PRFs.

changing the BC. The IEDs with the smaller BC extend to higher energy, reflecting the larger momentary V_S that occurs when the dc-bias cycles to more negative values during the *LF* pulse.

IEDs for O^+, Ar^+, and CF_3^+ are shown in Fig. 12 for different BCs when pulsing the *LF* with a PRF of 50 kHz. Due to its smaller mass, O^+ has a broader IED than Ar^+ and CF_3^+. Counter to what one would expect based only on their masses, the IED for Ar^+ is shifted toward lower energy in the tail of the IED compared to CF_3^+. This counterintuitive trend is likely due to the source functions for different ions having different time dependencies during the pulse period and being formed at different distances from the sheath edge.

The IEDs for all ions with different duty-cycles are shown in Fig. 13 when pulsing the *HF* power with a PRF of 50 kHz and with BCs of 10 nF and 1 μF. The dc-biases for these conditions are shown in Fig. 14. In all cases, with the onset of the *HF* pulse, the dc-bias increases to more positive values before settling to a more positive but still negative dc-bias. In the case of the smaller BC, the dc-bias actually momentarily becomes positive. When the *HF* power is terminated, the dc-bias returns to its initially more negative value as would be expected for single *LF* operation. Although the range in energy of the IEDs does not significantly change when changing the duty-cycle, the shapes of the IEDs are sensitive to duty-cycle. The range in energies results from the maximum and minimum values of $V_S = V_P - V_{dc}$, which does not significantly vary with duty-cycle. The details of the structure of the IEDs depend on the time variation of V_S, which does depend on duty-cycle.

The IEDs for all ions are shown in Fig. 15 for different duty-cycles when pulsing the *LF* power for a PRF of 50 kHz and for BCs of 10 nF and 1 μF. The dc-biases for these conditions are shown in Fig. 16. For these conditions, the dc-bias is positive when the *LF* is off (*cw HF*). When pulsing the *LF*, the dc-bias spikes to negative values. With the

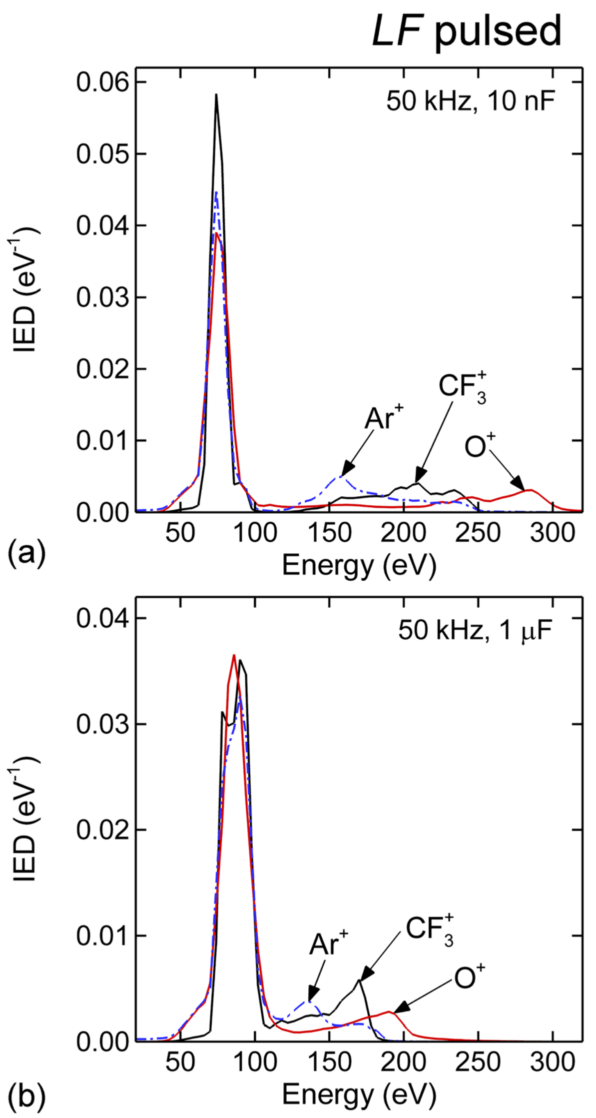

FIG. 12. (Color online) IEDs for O^+, Ar^+, and $CF_3{}^+$ when pulsing the *LF* power. (a) BC = 10 nF and (b) BC = 1 μF.

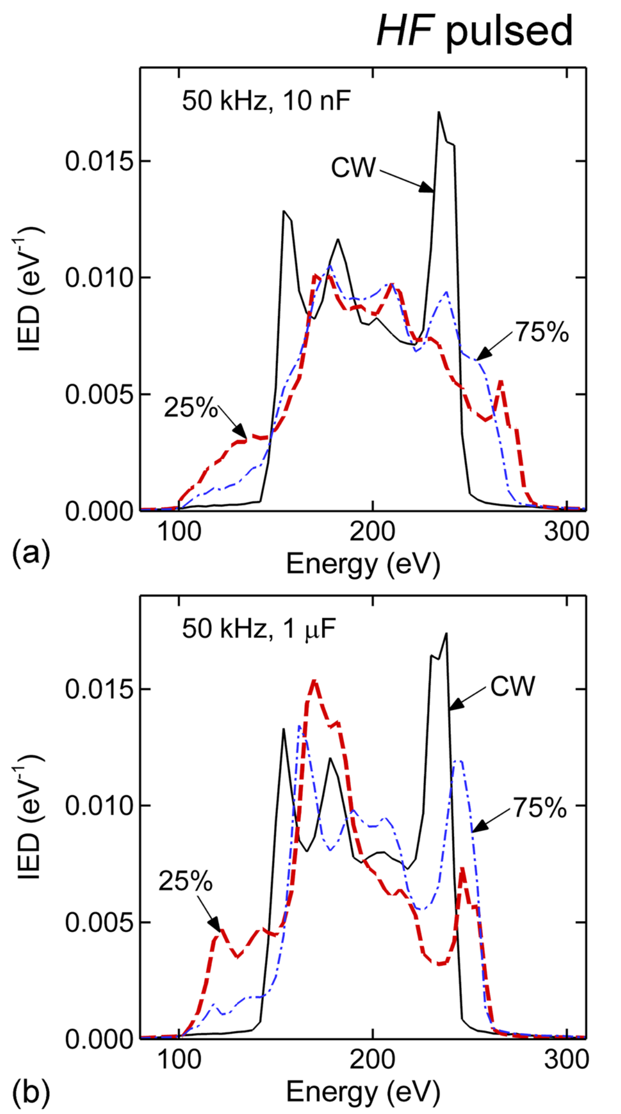

FIG. 13. (Color online) Total IEDs for all ions for different duty-cycles when pulsing the *HF* power with a PRF of 50 kHz. (a) BC = 10 nF and (b) BC = 1 μF. The *LF* power is *cw*. The smaller duty-cycle tends to produce an extended energy range in the IED.

smaller BC, the dc-bias during the *LF* power-on portion of the cycle is essentially the same as for *cw* operation and recovers back to positive values during the *LF* power-off portion of the cycle. With the smaller BC, the dc-bias is about the same value during the *LF* power-on (−40 V) and *LF* power-off (80 V) portions of the cycle. As a result, the low energy and high energy portions of the IEDs have the same structure and ranges of energies for different duty-cycles. By changing the duty-cycle, the proportion of the IED in the low energy and high energy ranges can be controlled. For example, since the low energy range of the IED is produced during the *LF* power-off portion of the cycle, its magnitude increases with smaller duty-cycle (longer power-off period). Since the high energy range of the IED is produced during the *LF* power-on portion of the cycle, its magnitude increases with larger duty-cycle (longer power-on period).

When pulsing the *LF*, the IEDs are quite sensitive to duty-cycle when using the larger BC. The larger BC averages the time variations in the dc-bias obtained with the smaller BC. For these conditions, the result is that the dc-bias appears to have a nearly constant value, varying by only 20–30 V, for each duty-cycle. The large the duty-cycle, the more negative the dc-bias becomes, approaching the *cw* value. These trends are reflected in the IEDs, as shown in Fig. 15(b). Larger duty-cycles produce IEDs which resemble those for *cw* excitation. Decreasing the duty-cycle produces a smaller V_S throughout the pulse period since the dc-bias is more positive, and this shifts the low energy peak of the IED to lower energies. The magnitude of the low energy peak increases with smaller duty-cycle. This trend results from the plasma potential being supported by only the *HF* during a larger fraction of the pulse period, and so $V_S = V_P - V_{dc}$ is at its minimum value for a longer fraction of the period.

V. CONCLUSIONS

The properties of IEDs in pulse powered DF-CCPs sustained in an $Ar/CF_4/O_2$ mixture have been computationally

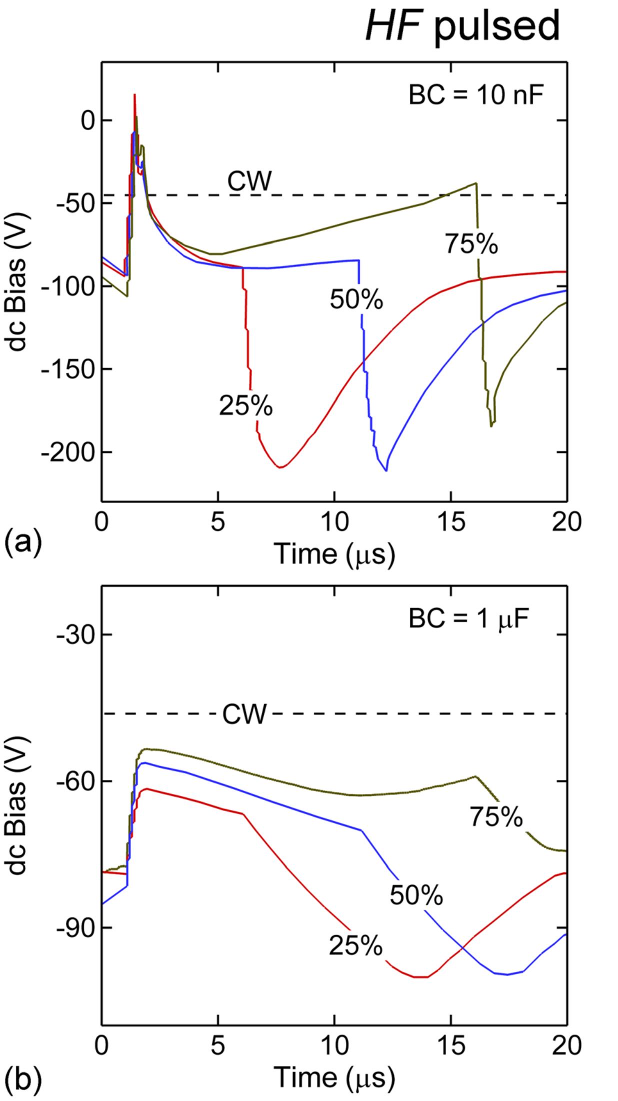

FIG. 14. (Color online) Temporal behavior of dc-bias with different duty-cycles when pulsing the *HF* power with a PRF of 50 kHz. (a) BC = 10 nF and (b) BC = 1 μF. The *LF* power is *cw*. The dynamic range of the dc-bias is from 0 V to −200 V with the smaller BC while the range is only from −60 to −90 V with larger BC.

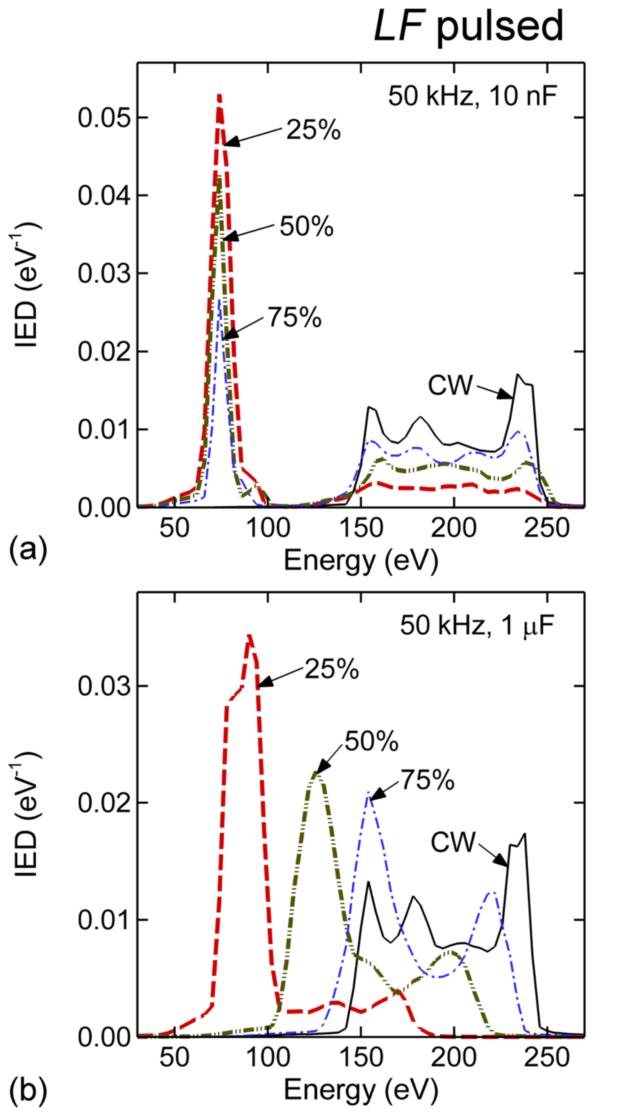

FIG. 15. (Color online) Total IEDs for all ions for different duty-cycles when pulsing the *LF* power with a PRF of 50 kHz. (a) BC = 10 nF and (b) BC = 1 μF. The *HF* power is *cw*. The amplitude of the low energy peak diminishes while the amplitude of the high energy peak increases as the duty-cycle increases. The IED becomes similar to that of the *cw* case with further increase of the duty-cycle.

investigated using results from a 2D plasma hydrodynamics model. We found that varying the size of the BC is an additional variable which provides flexibility in controlling the shape of the IEDs. The maximum ion energy tends to increase with smaller BC as the dc-bias travels through a larger dynamic range over the pulse period when pulsing either the *LF* or *HF*. When pulsing the *LF*, lower ion energies are preferentially produced during the power-off period of the *LF* when only the *HF* is on regardless of the size of the BC. When pulsing the *HF*, higher ion energies are preferentially produced during the power-on period of the *HF* regardless of the size of the BC. However, the dynamics and details of the shape of the IEDs depend on the value of the BC. The shape of the IED is further a function of the PRF and duty-cycle of the pulse period, and depends on whether the *LF* or *HF* is pulsed. When pulsing the *HF*, higher PRF and smaller duty-cycle tend to produce higher energy ions. When pulsing the *LF*, PRF does not have a large effect on the shape of the IED; however, duty-cycle does affect the shape of the IED, and more so with larger BC. The maximum values of ion energies are not necessarily monotonically dependent on, for example, PRF for a given BC since the IEDs depend on the details of the ion response to the Fourier components of the bias that result from the pulsing. These conclusions are based on the total IED for all ions —there is additional variation and control that depends on the individual masses of the ions. The individual spikes in the total IED can be correlated with the individual response of different ions to the Fourier components of the time variation in the dc-bias.

Our results also depend on the details of the matching networks used with the plasma tool. Our circuit model has purposely been chosen to be simple in order to make a direct connection between the change in the dc bias and the plasma properties. Having said that, commercial matching networks

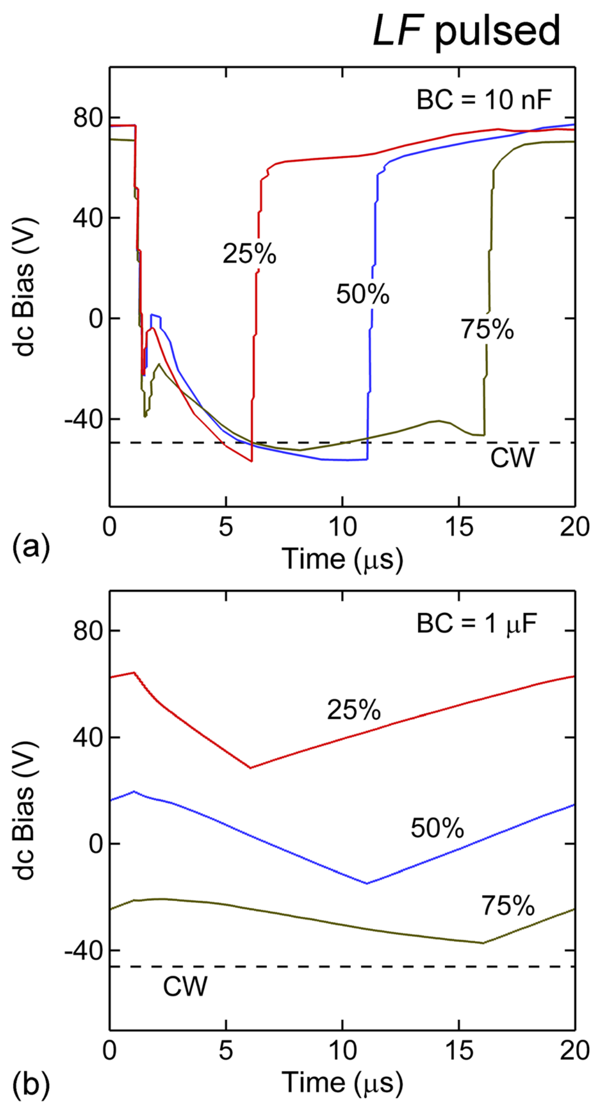

FIG. 16. (Color online) Temporal behavior of dc-bias with different duty-cycles when pulsing the *LF* power with a 50 kHz PRF. (a) BC = 10 nF and (b) BC = 1 μF. The *HF* power is *cw*. The dynamic range is from −40 to +80 V with the smaller BC while the range is at most ±15 V at 25% duty-cycle with larger BC. Note that the range of oscillation the dc-bias is similar for different duty-cycles with the smaller BC while the range is shifted by duty-cycle with the larger BC.

will attempt to compensate for the changing plasma impedance during the pulsed period, and part of that compensation may be to change the effective serial capacitance. To unambiguously control the IEDs, needs to be controlled, effective blocking capacitance, and this may compromise the ability to optimally match during pulsed operation.

ACKNOWLEDGMENTS

This work was supported by the Semiconductor Research Corp., Department of Energy Office of Fusion Energy Sciences, and the National Science Foundation.

[1]V. M. Donnelly and A. Kornblitt, J. Vac. Sci. Technol. A **31**, 050825 (2013).
[2]X. V. Qin, Y.-H. Ting, and A. E. Wendt, Plasma Sources Sci. Technol. **19**, 065014 (2010).
[3]S. H. Lee, P. K. Tiwari, and J. K. Lee, Plasma Sources Sci. Technol. **18**, 025024 (2009).
[4]A. Agarwal, S. Rauf, and K. Collins, J. Appl. Phys. **112**, 033303 (2012).
[5]A. Agarwal, P. J. Stout, S. Banna, S. Rauf, K. Tokashiki, J.-Y. Lee, and K. Collins, J. Appl. Phys. **106**, 103305 (2009).
[6]S. Samukawa, Appl. Phys. Lett. **64**, 3398 (1994).
[7]S. Banna *et al.*, IEEE Trans. Plasma Sci. **37**, 1730 (2009).
[8]P. Diomede, D. J. Economou, and V. M. Donnelly, J. Appl. Phys. **109**, 083302 (2011).
[9]R. Legtenberg, H. Jansen, M. de Boer, and M. Elwenspoek, J. Electrochem. Soc. **142**, 2020 (1995).
[10]H. M. Park, C. Garvin, D. S. Grimard, and J. W. Grizzle, J. Electrochem. Soc. **145**, 4247 (1998).
[11]A. C. Westerheim, A. H. Labun, J. H. Dubash, J. C. Arnold, H. H. Sawin, and V. Yu-Wang, J. Vac. Sci. Technol. A **13**, 853 (1995).
[12]G. S. Oehrlein, Y. Zhang, D. Vender, and O. Joubert, J. Vac. Sci. Technol. A **12**, 333 (1994).
[13]K. Maeshige, G. Washio, T. Yagisawa, and T. Makabe, J. Appl. Phys. **91**, 9494 (2002).
[14]T. Ohmori, T. Goto, and T. Makabe, J. Phys. D: Appl. Phys. **37**, 2223 (2004).
[15]M. J. Kushner, J. Phys. D **42**, 194013 (2009).
[16]D. L. Scharfetter and H. K. Gummel, IEEE Trans. Electron Devices **16**, 64 (1969).
[17]S. H. Song and M. J. Kushner, Plasma Sources Sic. Technol. **21**, 055028 (2012).
[18]Y. Zhang, M. J. Kushner, N. Moore, P. Pribyl, and W. Gekelman, J. Vac. Sci. Technol. A **31**, 061311 (2013).
[19]A. V. Vasenkov, X. Li, G. S. Oehrlein, and M. J. Kushner, J. Vac. Sci. Technol. A. **22**, 511 (2004).
[20]C. Bohm and J. Perrin, Rev. Sci. Instrum. **64**, 31 (1993).
[21]A. Agarwal, P. J. Stout, S. Banna, S. Rauf, and K. Collins, J. Vac. Sci. Technol. A **29**, 011017 (2011).